J Sol-Gel Sci Technol (2017) 82:2–14
DOI 10.1007/s10971-017-4339-6

INVITED PAPER: NANO- AND MACROPOROUS MATERIALS (AEROGELS, XEROGELS, CRYOGELS, ETC.)

Transparent polyvinylsilsesquioxane aerogels: investigations on synthetic parameters and surface modification

Taiyo Shimizu[1] · **Kazuyoshi Kanamori**[1] · **Kazuki Nakanishi**[1]

Received: 24 November 2016 / Accepted: 17 February 2017 / Published online: 6 March 2017

Abstract Systematic investigations on the effect of synthetic conditions onto the properties of polyvinylsilsesquioxane (CH_2=$CHSiO_{3/2}$) aerogels have been conducted. As previously reported, transparent polyvinylsilsesquioxane aerogels can be obtained by utilizing a liquid surfactant as a solvent and a two-step sol–gel reaction involving hydrolysis catalyzed by a strong acid and subsequent polycondensation by a strong base. In this study, effects of base catalyst, gelation and aging conditions, amount of surfactant and concentration of acid catalyst have been investigated. With the optimized synthetic condition, the value of light transmittance reaches as high as 70% (at the wavelength of 550 nm for a 10-mm thick sample). Applicability of addition reactions utilizing thiol-ene reactions and hydrosilylation has also been surveyed. Thiol-ene reactions are relatively effective and can modify surface hydrophobicity and mechanical properties of polyvinylsilsesquioxane aerogels. In the case of hydrosilylation, a partial addition of a hydrosilane compound onto the polyvinylsilsesquioxane gel surface can be observed. Addition reactions, in particular thiol-ene reactions, are found to be profitable for implementing chemical functionality on the transparent aerogels.

Graphical Abstract

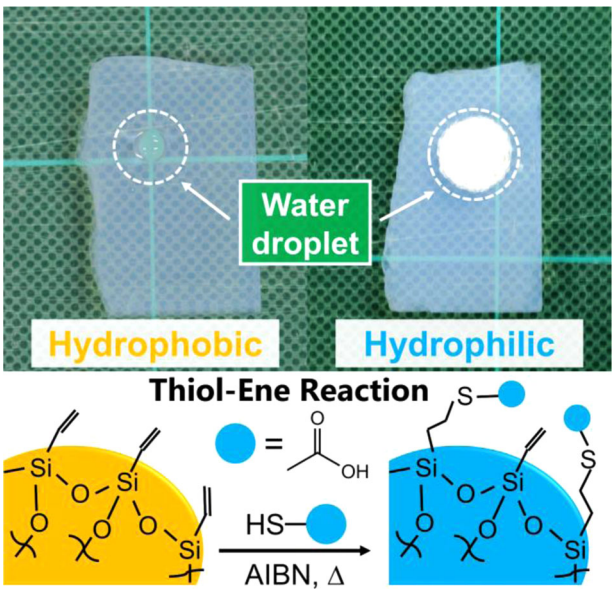

Keywords Polyvinylsilsesquioxane · Aerogel · Visible-light transparency · Thiol-ene reactions · Hydrosilylation

1 Introduction

Among various porous materials, silica aerogels are regarded as a special class of materials due to their unique properties. Characteristic properties such as low density, low thermal conductivity, high surface area, and high transparency for visible-light [1], are mostly derived from their unique pore structures in the nanometer scale, prepared by retaining skeletal structures of wet gels via drying under

Electronic supplementary material The online version of this article (doi:10.1007/s10971-017-4339-6) contains supplementary material, which is available to authorized users.

✉ Kazuyoshi Kanamori
kanamori@kuchem.kyoto-u.ac.jp

[1] Department of Chemistry, Graduate School of Science, Kyoto University, Kitashirakawa, Sakyo-ku, Kyoto 606-8502, Japan

supercritical conditions. Pores in size of ca. 50 nm with thin (10–20 nm) solid skeletons can suppress both visible-light scattering via the Mie [2] and Rayleigh modes [3], and heat transport by a gas phase inside the pore space [4], realizing the above properties. However, such tenuous pore structures also subject silica aerogels to low mechanical strength, which makes handling and reshaping of them difficult. Since even a small deformation especially by bending and stretching can fracture silica aerogels, an improvement of mechanical properties has been highly demanded. In that sense, organic–inorganic hybridization is a well-studied way to reduce the native brittleness of silica backbones [5]. In our recent works, transparent polymethylsilsesquioxane (PMSQ, $CH_3SiO_{3/2}$) aerogels have successfully been synthesized from a single precursor methyltrimethoxysilane, and a substantial improvement in mechanical strength has been achieved [6–8]. Since phase separation tendency between aqueous solvent and condensates formed from an organotrialkoxysilane increases in the course of polycondensation [9], the formation of a monolithic gel requires a well-designed synthetic procedure so as to suppress the phase separation and enhance the network formation. In most cases, the phase separation proceeds to form macroscopic double phase of polar solvents and alkoxysilane-derived oil or resin [10], or even if a monolithic gel can be formed, the resultant gel will be opaque due to coarsened pore structures in micro- or submicrometer scales [11]. In our synthetic strategy, effective suppression of phase separation has been accomplished by employing a modified two-step acid-base sol–gel reaction in the presence of surfactant. Although it had already been reported that two-step acid-base reactions are effective to prepare monolithic gels in the PMSQ system [12], both the presence of surfactant and homogeneously increasing pH in the whole system by hydrolysis of urea can produce highly transparent gels. In addition to improved flexibility and resilience against compression, resultant PMSQ aerogels show high transparency and low thermal conductivity comparable to those of silica counterparts [13, 14]. This success in the suppression of phase separation between hydrophobic organopolysiloxane condensates and aqueous solvents is potential for opening up new functionalities in transparent aerogels not only for mechanical improvement.

More recently, our group has also reported a synthesis of transparent polyvinylsilsesquioxane (PVSQ, $CH_2{=}CHSiO_{3/2}$) aerogels [15]. The newly developed synthetic procedure, which utilizes a liquid surfactant as a part of solvent and strong acid and base as the catalyst for hydrolysis and polycondensation, respectively, can effectively suppress phase separation tendency between highly hydrophobic PVSQ condensates and solvents, leading to the formation of transparent gels. In addition, pendant vinyl groups in the PVSQ network display reactivity to radical polymerization even in the preformed solid matrix, resulting in additional crosslinking by polymerized vinyl groups between polysiloxane networks, similar to "vulcanization" in silicone chemistry [16]. With an increasing concentration of radical initiator in the post-treatment, the vulcanized PVSQ aerogels show higher compressive stress against uniaxial compression and higher resilience after removal of load, while retaining their transparency. Through 44% of vinyl groups reacted at maximum, this mechanical improvement can also produce transparent and low-density aerogel-like xerogels, which are obtained by evaporative drying instead of supercritical drying. Such reactivity of vinyl groups in the scaffold is considered to be advantageous to implement functionality on transparent aerogels via chemical modifications utilizing addition reactions.

Here, we report on the effect of synthetic conditions onto the various properties of resultant PVSQ aerogels in detail, particularly focusing on their transparency. On the basis of the previously-reported synthetic condition [15], investigation on the effects of base catalyst, aging conditions, amount of surfactant, and acid concentration has been carried out, in order to optimize the synthetic condition for highly transparent aerogels. Moreover, we have also investigated the availability of post-modification of skeletal surface using thiol-ene reactions and hydrosilylation. A high efficiency of these addition reactions is desired for imparting chemical functionalities to these transparent PVSQ aerogels.

2 Experimental section

2.1 Materials

Vinyltrimethoxysilane (VTMS) was purchased from Shin-Etsu Chemical Co. (Japan). Aqueous nitric acid (60%), lithium hydroxide monohydrate, sodium hydroxide, potassium hydroxide, methanol, 2-propanol, and toluene were purchased from Kishida Chemical Co., Ltd. (Japan). Distilled water was purchased from Hayashi Pure Chemical Ind., Ltd. (Japan). Surfactant polyoxyethylene 2-ethylhexylether (Nonion EH-208) was kindly donated from NOF Corporation (Japan). Aqueous tetraethylammonium hydroxide (TEAOH) (35 wt%), tetrapropylammonium hydroxide (TPAOH, 1.0 M), and platinum(0)-1,3-divinyl-1,1,3,3,-tetramethyldisiloxane complex solution (Karstedt's catalyst, ca. 2% in xylene) were purchased from Sigma-Aldrich Japan. Aqueous tetramethylammonium hydroxide (TMAOH, ca, 25%), choline hydroxide (48–50%), tris(2-hydroxyethyl)methylammonium hydroxide (THMAOH) (45–50%, stabilized with 4-methoxyphenol), 2,2′-azobis(isobutyronitrile) (AIBN), thioglycolic acid (TGA), thiolactic acid (TLA),

2-aminoethanethiol (AET), 4-aminobenzenethiol (ABT), 1,2-ethanedithiol (EDT), 1,3-propanedithiol (PDT), 1,4-butanedithiol (BDT), and triphenylsilane (TPS) were purchased from Tokyo Chemical Industry Co., Ltd. (Japan). All the chemicals were used without further purification.

2.2 Preparation of PVSQ aerogels

The synthetic procedure for a PVSQ gel is almost identical to the previous report [15]. Synthetic conditions of all PVSQ gels employed in the present study were systematically changed relative to the standard sample, PVSQ-sta as explained below. The synthetic procedure of a PVSQ-sta gel is as follows: First, VTMS (5.0 mL, 32.6 mmol) and 5 mM nitric acid (5.0 mL) were stirred together in a sealed glass vial for 6 min in order to promote hydrolysis of the methoxy groups. Surfactant EH-208 (6.0 mL) was then added to the mixture and the glass vial was transferred into an ice bath, in order to avoid the too fast reaction of subsequent polycondensation under a basic condition. After 3 min stirring, 0.60 M TMAOH (2.0 mL) was added to the reaction solution and stirred for 3 min. Then the reaction solution was transferred to a polystyrene container and rested in a refrigerator at 4 °C, followed by gelation. After gelation, the container was transferred in an oven at 40 °C and the gel was aged for 4 days in order to promote polycondensation of silanol groups. During this aging step, the gel surface was covered with methanol 1 day after the start of aging at 40 °C, in order to prevent cracks generated during the following washing processes. The obtained gel was further aged in water at 60 °C for 1 day. Subsequently, the gel was immersed in alcohols at 60 °C for at least 8 h, in order to get rid of unnecessary compounds in pore liquid. This washing process was conducted using methanol first and then 2-propanol, and each was repeated for three times. The obtained gel containing 2-propanol as pore liquid is referred to as alcogel. Obtained alcogels were supercritically dried at 14 MPa and 80 °C for 10 h under a CO_2 flow at 20 mL min^{-1}.

2.3 Thiol-ene reaction

Thiol-ene click reactions on PVSQ gels were conducted as follows: A PVSQ-sta alcogel (ca. 18 cm^3, containing 32.6 mmol of vinyl groups) containing 2-propanol as pore liquid was immersed in the solution comprising AIBN (1.0 g, 6.1 mmol), thiol (32.6 mmol) and 2-propanol (100 mL). After Ar bubbling for 5 min, the gel was rested at room temperature for 1 day, in order to diffuse AIBN and thiol into the whole pore liquid. The gel was then transferred into an oven at 60 °C and left to stand for 1 day. The obtained gel was washed with 2-propanol for three times, and supercritically dried.

2.4 Hydrosilylation

A PVSQ-sta alcogel (ca. 2.75 cm^3 in volume) was immersed in fresh toluene at 60 °C for at least 8 h, and this step was repeated for three times, in order to replace the pore liquid with toluene completely. Then, the wet gel was immersed in the solution, composed of Karstedt's catalyst solution in xylene (ca. 2%, 0.40 mL), TPS (1.297 g, ca. 1.0 equiv.) and toluene (20 mL), at 80 °C for 7 days. Subsequently the obtained gel was washed with 2-propanol for three times, and then supercritically dried.

2.5 Characterization

2.5.1 Visible-light transparency

Transparency of aerogels was measured by using a V-670 UV–Vis-NIR spectrophotometer (JASCO Corporation, Japan) equipped with an integrating sphere. Direct-hemispherical transmittance was measured and converted the value at the wavelength of 550 nm into that corresponding to a 10 mm thick-sample according to the Lambert–Beer equation.

2.5.2 Thermogravimetric analysis

Thermogravimetry and differential thermal analysis (TG-DTA) under atmospheric conditions was conducted by using Thermo plus EVO TG 8120 (Rigaku Corporation, Japan). Heating rate and flow rate of air were fixed at 5 °C min^{-1} and 100 mL min^{-1}, respectively. Obtained TG-DTA curves are shown in Fig. S1.

2.5.3 Mechanical properties

Uniaxial compression–decompression tests were carried out by using a material tester EZGraph (Shimadzu Corporation, Japan). Samples were reshaped with a razor into square cuboids of typically $10 \times 10 \times 5$ mm^3 in advance. Compression tests were conducted at 0.50 mm min^{-1} crosshead speed until the compressive strain reached at 50%, and then the crosshead was raised at the same rate.

2.5.4 Gas adsorption measurement

Nitrogen adsorption–desorption isotherms were obtained by using BELSORP-max (MicrotracBEL Corp., Japan). Before measurement, samples (ca. 0.020 g) were degassed in a sample cell under vacuum at 80 °C for 24 h. Measurement was carried out at 77 K. Obtained isotherms are displayed in Fig. S2.

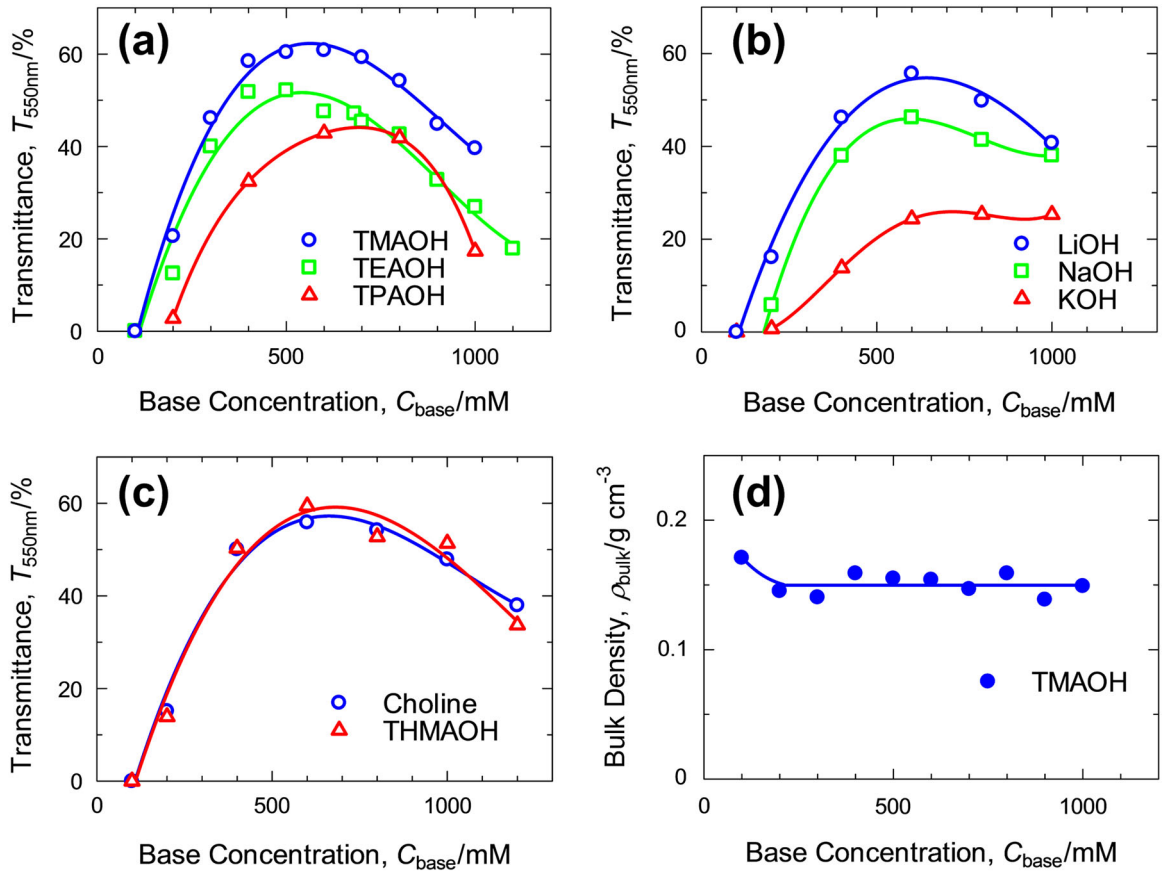

Fig. 1 Relationship between light transmittance (corresponding values to those of 10 mm-thick samples) and concentration of base catalyst, **a** tetraalkylammonium hydroxides, **b** alkali metal hydroxides, **c** hydroxyalkylammonium hydroxides. **d** Relationship between bulk density and the concentration of TMAOH

2.5.5 Molecular structure analysis

Fourier transform infrared (FT-IR) spectroscopy was carried out by using a spectrophotometer IRAffinity-1 (Shimadzu Corporation, Japan) equipped with an attenuated total reflection unit MIRacle A (PIKE Technologies, USA). Samples were ground into powder with a mortar and a pestle, and placed under vacuum at 80 °C for at least 1 h in advance of measurement. Raman spectra were obtained by a Raman microscope XploRA (HORIBA, Ltd., Japan). The wavelength of incident laser beam was 532 nm.

3 Results and discussion

3.1 Effect of base catalyst

Effects of the concentration and cation species of base catalyst on the transparency of resultant aerogels were investigated first. As already shown in the previous report [15], the concentration of base catalyst solution strongly affects the optical properties of obtained aerogels. Furthermore, it was also found that less transparent PVSQ gels are obtained when using tetraethylammonium hydroxide instead of tetramethylammonium hydroxide as the base catalyst. We thus focused on the effect of the kind of base catalyst in this study. Figure 1a–c displays the relationships between light transmittance and the concentration of base catalyst with several kinds of strong base, tetraalkylammonium hydroxides, alkali metal hydroxides, and hydroxyalkylammonium hydroxides. Obviously, these graphs show some distinct tendencies on transparency. Light transmittances of all of the obtained PVSQ aerogels increase in the low concentration region and show the highest values at ca. 500–600 mM, and then decrease with increasing concentration. This tendency is irrespective of the species of cations. On the other hand, the values of transmittance are strongly dependent on the types of cations. In the case of tetraalkylammonium hydroxides and alkali metal hydroxides, light transmittance increases in the order of TPAOH < TEAOH < TMAOH, and KOH < NaOH < LiOH, as observed in Fig. 1a, b. There is a clear tendency that smaller cations result in higher light transparency of resultant aerogels. Concerning two

Table 1 Properties of PVSQ aerogels gelled and aged for 4 days at different temperatures

Sample name	T_{gel} (°C)[a]	T_{age} (°C)[b]	$T_{550\,nm}$ (%)[c]	ρ_{bulk} (g cm^{-3})[d]	S_{BET} (m^2 g^{-1})[e]	t_{gel} (min)[f]
PVSQ-4-4	4	4	8.3	0.26	500	141
PVSQ-40-40	40	40	52	0.15	481	16
PVSQ-50-50	50	50	48	0.15	423	11
PVSQ-60-60	60	60	32	0.14	391	8
PVSQ-50-40	50	40	52	0.15	459	NA
PVSQ-60-40	60	40	50	0.15	454	NA

[a] Gelation temperature

[b] Aging temperature

[c] Light transmittance at 550 nm, normalized into the value of 10 mm-thick sample, using the Lambert-Beer equation

[d] Bulk density

[e] Brunauer-Emmett-Teller (BET) specific surface area obtained from nitrogen adsorption isotherms

[f] Gelation time

hydroxyalkylammonium cations (choline hydroxide and THMAOH), transparency of the aerogels prepared with these bases shows similar tendency to that of TMAOH (Fig. 1c). Choline hydroxide and THMAOH possess relatively large 2-hydroxyethyl groups, the number of which is 1 and 3, respectively. To elucidate the effects of cation species, complicated molecular-level interactions between the cation, condensate, water and EH-208 must be taken into account. In particular, compatibility of ionic pairs of the cation and silanolate groups on the condensates in the whole reaction system would give dominant influences on the resultant pore structure. The smaller and hydrophilic cation species with moderate interactions both with water and EH-208 are profitable for obtaining higher transparency as a general tendency. Figure 1d shows the transition of bulk density of aerogels with an increasing concentration of TMAOH. Except for $C_{TMAOH} = 100$ mM, bulk densities are almost constant irrespective of the concentration of TMAOH. Since no obvious shrinkage during supercritical drying can be observed in all PVSQ aerogels, the slightly high bulk density at 100 mM is attributed to relatively large syneresis that is presumably caused by a relatively loose network formation under the less basic condition. Even after gelation, there are still a lot of silanol groups remained, and relatively intensive polycondensation after aging causes large syneresis. From these results, it is important to select the appropriate concentration and cation species of base catalyst so that transparent and low-density PVSQ aerogels can be obtained.

3.2 Effect of gelation and aging conditions

We subsequently investigated effects of gelation and aging temperature on the properties of resultant PVSQ aerogels. A decrease in light transmittance was observed when gelation temperature (not aging temperature) was increased from 4 to 40 °C in the previous report [15]. Increasing gelation temperature gives rise to faster gelation, which may cause inhomogeneity in the formed pore structures, leading to the decrease in transparency. In order to investigate effects of gelation temperature, the properties of aerogels gelled and aged at 4, 40, 50, and 60 °C were compared first. Sample names, synthetic conditions and properties of the aerogels are listed in Table 1. In terms of light transmittance, PVSQ-4-4, which was gelled and aged at the lowest temperature among them, shows the lowest value. By contrast, increasing temperature from 40 to 60 °C gradually decreases the transmittance of resulting aerogels. In the case of PVSQ-4-4, aging temperature is too low to promote sufficient polycondensation between silanol groups, which results in large shrinkage (and thus high bulk density) derived from polycondensation of residual silanol groups during supercritical drying [17], and low transparency. The similarly large shrinkage during drying, due to insufficient aging, was also observed in polyethylsilsesquioxane ($CH_3CH_2SiO_{3/2}$) systems in the previous report [15]. In the range from 40 to 60 °C, no obvious shrinkage was observed during supercritical drying. Thus, these differences in transparency are originated from the temperature of gelation and/or aging. Figure 2a–c show pore structures of PVSQ-40-40, PVSQ-50-50 and PVSQ-60-60 in the nanometer scale. There are some differences in macroscopic transparency; however, no significant difference can be observed in the pore structures. The decrease in transparency is thus presumably derived from local inhomogeneity of pore structure, mainly caused by the fast gelation at high gelation temperature, and/or slight coarsening of the pore structure, derived from more intensive dissolution-reprecipitation reactions at higher aging temperature, both of which are difficult to be judged from these FE-SEM images. In order to discuss, whether gelation or aging temperature contributes to the decrease in light transmittance, PVSQ-50-40

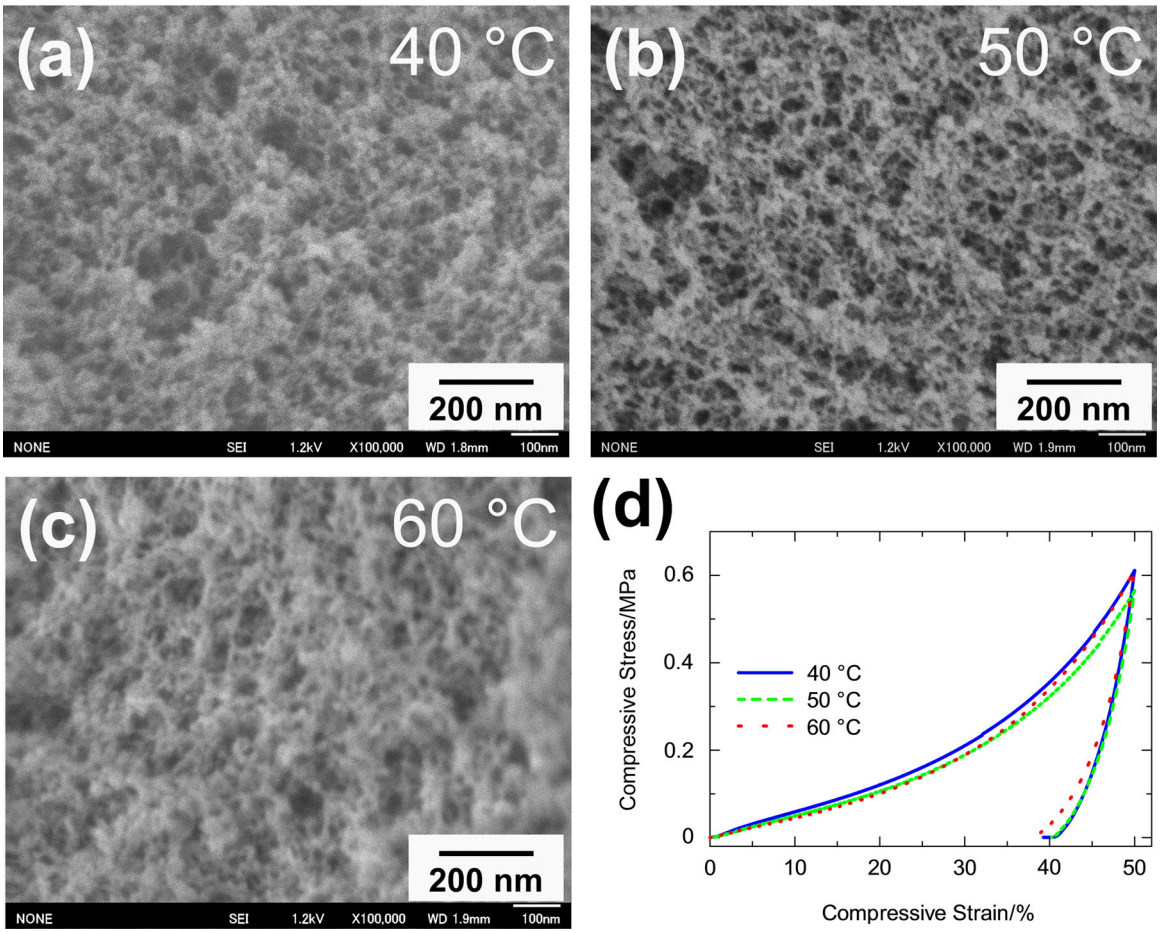

Fig. 2 a–c Field emission scanning electron microscope (FE-SEM) images, **d** stress–strain curves obtained from uniaxial compression–decompression tests on the aerogels gelled and aged at 40, 50, and 60 °C

and PVSQ-60-40 were also prepared. Both light transmittance and surface area of PVSQ-50-40 and PVSQ-60-40 show similar properties to those of PVSQ-40-40, and this result suggests that gelation temperature negligibly influences those properties. Aging at higher temperature promotes the dissolution-reprecipitation reactions on solid skeletons [18] and coarsens the pore structure, which decrease light transmittance and BET surface area. Thus, the difference in transmittance of PVSQ-40-40, PVSQ-50-50, and PVSQ-60-60 are mainly derived from aging temperature. Nitrogen adsorption–desorption isotherms shown in Fig. S2a support this interpretation. The onset of steep uptake around relative pressure $p/p^\circ = 0.9$, due to the capillary condensation of nitrogen gas in mesopores, is slightly shifted rightward as gelation and aging temperature increases. This roughly indicates that pore size increases with increasing gelation and aging temperature, although the shrinkage induced by the capillary condensation must be taken into account [19]. In terms of gelation temperature, the lower temperature may contribute to decrease local inhomogeneity in the pore structure due to a moderate gelation rate and increase transparency (transmittance of PVSQ-sta, gelled at 4 °C shows the highest, ca. 61%). However, there seems to be no substantial effect on the properties of aerogels in the range from 40 to 60 °C, due to the fast gelation (at 40 and 60 °C, gelation time is decreased by a factor of 9 and 18, respectively, compared to that of at 4 °C). Mechanical properties of PVSQ-40-40, PVSQ-50-50, and PVSQ-60-60 were also investigated. Stress–strain curves obtained from uniaxial compression–decompression are shown in Fig. 2d. In the previously reported ethylene-bridged polymethylsiloxane aerogels prepared with a similar procedure to the present work [20], gelation temperature substantially affects the compressive behaviors of resultant aerogels. In spite of the difference in gelation and aging conditions, however, these three aerogels show similar compressive stress at 50% strain and resilience after unloaded. These compressive stress and resilience are also similar to those in the previous report [15]. These results imply that when no shrinkage takes place during drying,

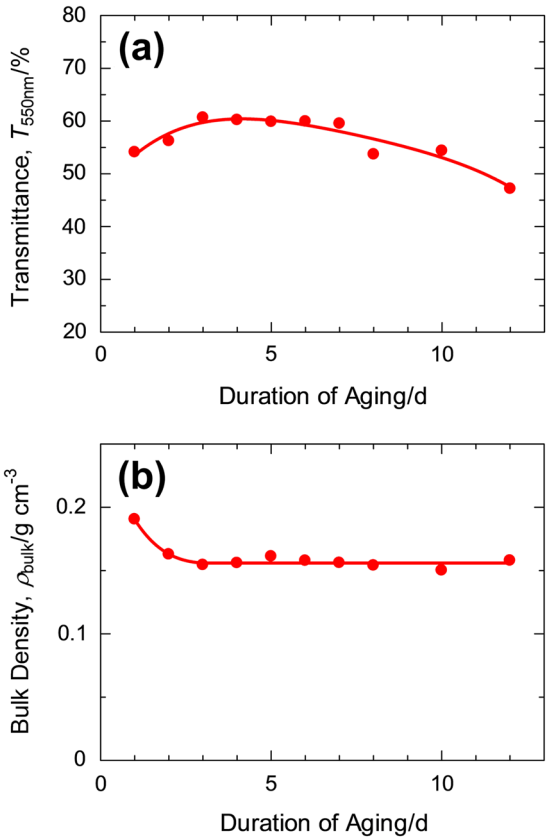

Fig. 3 **a** Light transmittance, **b** bulk density of aerogels with different duration of aging at 40 °C

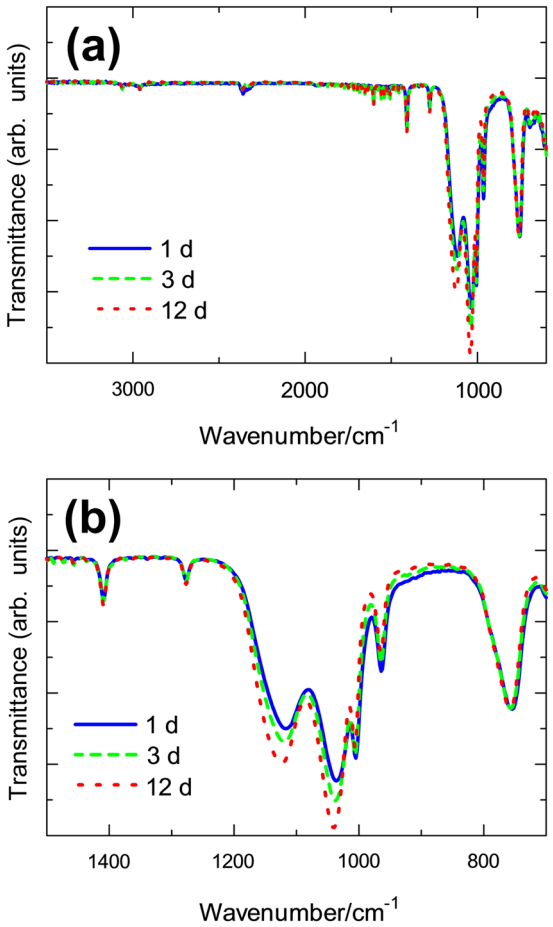

Fig. 4 **a** Full length, **b** selected area of FT-IR spectra of PVSQ aerogels with different duration of aging at 40 °C

which means that the obtained aerogels are sufficiently aged, even more intense aging conditions will not lead to an improvement of mechanical properties but end up only in decreasing the light transmittance of resultant aerogels. It seems to be difficult to achieve further improvement of resilience on compression only by changing the aging conditions.

Effects of aging duration are next discussed. Figure 3 shows the relationship between the duration of aging and light transmittance and bulk density. Up to 3 days of aging, light transmittance of aerogels increases with an increasing duration of aging. Longer aging allows the transmittance value to stay almost constant up to ca. 6–7 days, and then gradually decreases. This tendency can be attributed to the progress of aging of the gel skeletons. As shown in Fig. 3b, bulk density decreases until 3 days with increasing duration of aging, and then shows almost constant values. As observed in PVSQ-4-4, aging for less than 3 days produces insufficiently aged gels, which show larger shrinkage during supercritical drying and result in higher bulk density and lower transparency. Enhanced polycondensation during aging can be observed in FT-IR spectra shown in Fig. 4; the absorption bands at 1040 and 1123 cm^{-1}, corresponding to the Si−O−Si bonds [21], are increased. The decrease in transmittance after 6–7 days is derived from coarsening due to the extended aging. It can be confirmed that BET surface area of aerogels monotonously decreases with the increasing duration of aging (duration of aging = 1, 3, 8, and 12 days: $S_{BET} = 519$, 493, 429, and 390 m^2 g^{-1}), and thus, further coarsening of the pore structure is considered to proceed due to the dissolution-reprecipitation of solid skeletons. A similar tendency is also observed when a silica gel is aged in water at 40–100 °C [22]. From above results, it is found that appropriate conditions of gelation and aging such as temperature and duration (e.g. for 4 days at 40 °C) are necessary to obtain transparent aerogels.

3.3 Effect of the amount of EH-208

Subsequently, we investigated effects of the amount of EH-208 on the properties of resultant aerogels. Figure 5 shows the relationship between the volume of EH-208 in the starting composition and light transmittance and bulk density. As observed in Fig. 5a, light transmittance first increases with the increasing amount of EH-208 and reaches

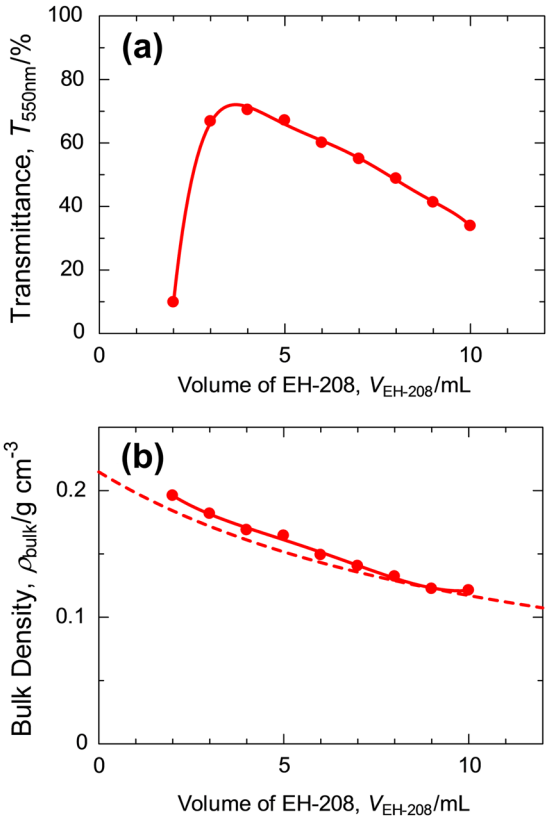

Fig. 5 Relationship between the volume of EH-208 and **a** light transmittance, **b** bulk density of aerogels. A *dashed line* displays the ideal bulk density, which is calculated by assuming that there is no shrinkage during the whole process, ideal conversion from VTMS into PVSQ, and no volume change by mixing

the maximum of 70%, and then decreases. When $V_{EH-208} =$ 1 mL, macroscopic phase separation took place and monolithic gel could not be obtained. An increasing amount of EH-208 up to $V_{EH-208} = 4$ mL contributes to suppress the phase separation tendency between the PVSQ condensates and solvents, and resultant aerogels became more transparent. Above that, light transmittance gradually decreases due to dilution of the precursor, which disturbs the formation of fine and homogeneous pore structures. Figure 5b shows the transition of bulk density with respect to the amount of EH-208. The dashed line exhibits ideal bulk density, where no shrinkage during the whole process, complete conversion from VTMS into PVSQ, and no volume change by mixing are assumed. The measured bulk density gradually approaches the ideal one with the increasing amount of EH-208. This behavior can be attributed to less syneresis after gelation in more diluted conditions. In such cases, a less concentration of reactive sites for polycondensation (silanols) remains at the onset of gelation, leading to less syneresis. In other words, gelation can take place with a lower degree of condensation in less diluted conditions, which leads to a higher degree of syneresis. In order to obtain highly transparent aerogels, the amount of EH-208 should be in the region in $V_{EH-208} = 3$–5 mL. The aerogel obtained with $V_{EH-208} = 4$ mL shows the highest light transmittance (70%) with retaining relatively low bulk density (0.17 g cm^{-3}), while no apparent changes in the compressive mechanical properties can be observed (Fig. S3).

3.4 Effect of acid concentration

As compared to the base catalyst, effects of the concentration of nitric acid on the properties of resultant aerogels are considered to be minor, due to the short duration (6 min) of being under acidic conditions. However, polycondensation of silanol groups actually proceeds even under dilute acidic conditions. Mixing of the same volume of 5 mM nitric acid and VTMS produces a homogeneous solution after 1–2 min due to the hydrolysis of methoxy groups, and after 30–40 h at room temperature, the solution undergoes macroscopic phase separation into two phases of an aqueous solution and viscous oil. The viscous oil is presumably composed of cyclic compounds or oligomeric/polymeric derivatives generated by polycondensation under acidic conditions, as frequently observed in similar organotrialkoxysilanes [10]. Thus, we investigated effects of acid catalyst. In order to realize similar pH conditions at gelation to that of PVSQ-sta, four aerogels were prepared with higher concentrations of nitric acid and TMAOH, taking only the neutralization between these two into account. Sample names and properties of aerogels are listed in Table 2. Obviously, the light transmittance of aerogels decreases with the increasing concentration of both nitric acid and TMAOH. This decrease can be related to the increase in the concentration of electrolytes in the reaction solution. In a reaction system, where phase separation may be induced by the progress of polymerization in an aqueous solution [9], the dispersion stability of the growing colloidal particles becomes one of the dominant parameters that affect the resultant pore structure in parallel with the phase separation. In particular, where the volume fraction of the gelling phase is relatively low like in the present PVSQ systems, the resulting pore structure would be highly sensitive to the tendency of colloidal aggregations. The increase in the concentration of electrolytes (tetramethylammonium and nitrate ions) disturbed the electrostatic stability of colloidal particles [23], resulting in an enhanced degree of aggregation and lowered transmittance. The shortened gelation times (from 141 min for PVSQ-4-4, to 32 min for PVSQ-560-2000) support this interpretation. A similar decrease in light transmittance is also observed when only the concentration of nitric acid is altered (Fig. S4). The measured light transmittance is lower than the expected values taking only the neutralization of

Table 2 Properties of PVSQ aerogels obtained with keeping the pH conditions at gelation similar to that of PVSQ-sta

	C_{NA} (mM)[a]	C_{TMAOH} (mM)[b]	T_{550nm} (%)	ρ_{bulk} (g cm^{-3})	t_{gel} (min)
PVSQ-560-2000	560	2000	30	0.14	32
PVSQ-360-1500	360	1500	37	0.14	39
PVSQ-160-1000	160	1000	49	0.15	58
PVSQ-80-800	80	800	55	0.15	88

[a] Concentration of nitric acid

[b] Concentration of TMAOH

nitric acid by TMAOH into account. For instance, when the concentrations of nitric acid and TMAOH are 100 mM (5 mL) and 600 mM (2 mL), respectively, the expected value of transmittance from the curve in Fig. 1a is ca. 50%, corresponding to the concentration of TMAOH of 350 mM (600 mM − 100 mM × (5 mL ÷ 2 mL)), assuming the concentration of nitric acid employed in Fig. 1a (5 mM) is negligible. However, the measured value of transmittance was 41%. This decrease in transmittance is also derived from the increase in the concentration of the electrolyte, nitrate ion. In terms of molecular structures, FT-IR spectra of PVSQ-560-2000, PVSQ-80-800 and PVSQ-sta are shown in Fig. 6. There is no clear difference between these aerogels even in the region of siloxane networks around 1040 and 1123 cm^{-1}, corresponding to linear/branched and polycyclic structures, respectively [24]. In the case of previously reported PMSQ systems using weak acid and weak base as catalysts, using a high concentration of acid results in the molecular structure containing more polycyclic parts [25]. However, under highly basic conditions for polycondensation in this study, the preferentially formed cyclic structures may undergo cleavage and rearrangement of siloxane bonds, and the whole molecular structure reaches an equilibrium between linear/branched and polycyclic structures. From above results, the concentration of nitric acid is desired to be minimum for hydrolysis to proceed smoothly in order to obtain transparent aerogels.

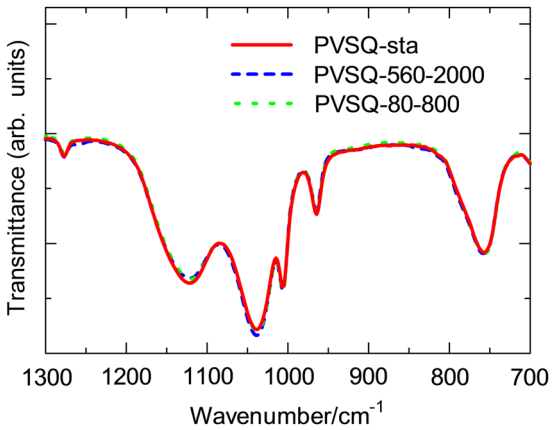

Fig. 6 FT-IR spectra of PVSQ-sta, PVSQ-560-2000 and PVSQ-80-800 in the region related to siloxane network

3.5 Thiol-ene click reactions

We subsequently attempted chemical modifications on the surface of PVSQ aerogels by using thiol-ene click reactions [26]. This chemical modification process was utilized not only in the synthesis of the precursor [27], but also surface modification via post treatments [28, 29] for porous silicone-based materials, and thus, it is a promising way to functionalize the surface of PVSQ aerogels. Sample names and their properties are listed in Table 3. First, changes in surface properties by the addition reaction of thiols with polar substituent groups, such as carboxyl and amino, were investigated. Figure 7a and b show the appearance of PVSQ-sta and PVSQ-TGA aerogels after dropping of distilled water (ca. 0.03 mL), respectively. The surface of PVSQ-sta is highly hydrophobic and completely repels the water droplet. By contrast, the water droplet on PVSQ-TGA permeated through the surface and collapsed the pore structure, resulting in the opaque appearance. This result can be attributed to the polar carboxylic group. The imparted carboxylic acid increases the hydrophilicity of solid skeletons and wetting of skeletal surface by water takes place. Figure 6c shows FT-IR spectra of the both aerogels. While the absorption bands at 1603, 1410, and 964 cm^{-1}, corresponding to C=C bond [21, 30], decrease after the thiol-ene reaction, a new band at 1720 cm^{-1} emerges. This peak is characteristic of C=O in the carboxyl groups, and thus the reaction between vinyl groups and TGA was considered to successfully proceed. Similar changes in hydrophobicity/hydrophilicity and FT-IR spectra were also observed when TLA and AET were employed as a reagent. Both PVSQ-TLA and PVSQ-AET show hydrophilicity and a decrease in the absorption corresponding to C=C bonds in FT-IR spectra (Figs. S5 and S6), although absorption bands corresponding to amino groups cannot be clearly observed in Fig. S6. In the case of ABT, the addition reaction cannot be confirmed to take place, because there is no difference between transparency, bulk density, hydrophobicity and FT-IR spectra (Fig. S7) of both aerogels.

Table 3 Properties of PVSQ aerogels treated with thiol-ene click reactions

Sample name[a]	Thiol	T_{550nm} (%)	ρ_{bulk} (g cm^{-3})	Yield (%)[b]	S_{BET} (m^2 g^{-1})	Hydrophobic or hydrophilic[c]
PVSQ-TGA	Thioglycolic acid	39	0.20	38	348	Hydrophilic
PVSQ-TLA	Thiolactic acid	49	0.18	25	429	Hydrophilic
PVSQ-AET	2-Aminoethanethiol	46	0.18	20	405	Hydrophilic
PVSQ-ABT	4-Aminobenzenethiol	61	0.16	0	493	Hydrophobic
PVSQ-EDT	1,2-Ethanedithiol	38	0.18	15	381	NA
PVSQ-PDT	1,3-Propanedithiol	41	0.18	24	376	NA
PVSQ-BDT	1,4-Butanedithiol	34	0.19	19	374	NA

[a] All of the samples were prepared from PVSQ-sta alcogels

[b] Estimated from weight loss at 800 °C in thermogravimetry, assuming complete conversion into a pure silica

[c] Determined from wettability of distilled water

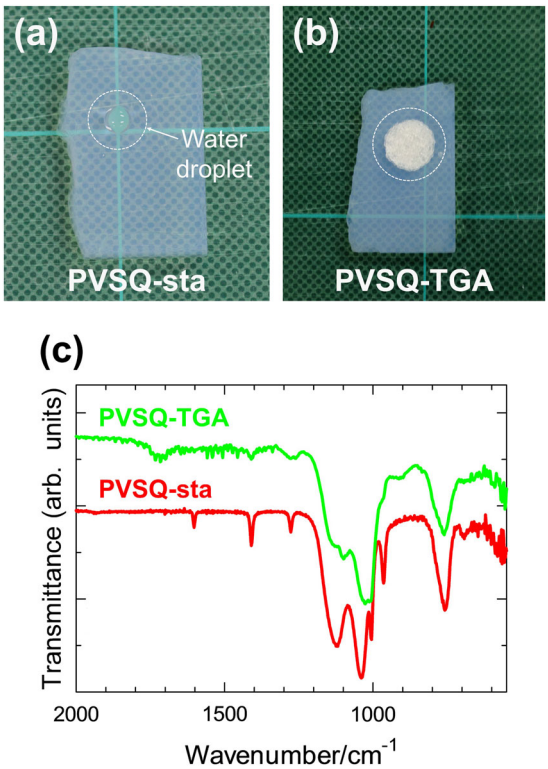

Fig. 7 Appearance after dropping distilled water (ca. 0.03 mL) onto **a** PVSQ-sta, **b** PVSQ-TGA aerogel. Water dropped onto PVSQ-TGA instantly permeated to the surface and collapsed it, resulting in the opaque appearance due to light scattering. **c** FT-IR spectra of both aerogels

Concerning PVSQ-TGA, PVSQ-TLA and PVSQ-AET, surface areas of these aerogels are lower than typical PVSQ aerogels (The highest value is 541 m^2 g^{-1}, reported in [15].), however, there are still substantial surface areas remaining. These successful surface modifications are promising for applications such as gas sorbent [31, 32].

Forming new crosslinks between vinyl groups by thiolene reactions using dithiols was also attempted. As aforementioned in Introduction, improvements of mechanical properties (elastic modulus and resilience after compression–decompression) in PVSQ systems have already been achieved by radical polymerization of vinyl groups in the network. In the present study, another approach for crosslinking between vinyl groups using dithiols with different length of alkyl chains, 1,2-EDT, 1,3-PDT, and 1,4-BDT, was employed. Efficiency of creating new crosslinks on improving resilience of aerogels using such as epoxy [33] and styrene [34] onto specific reactive sites was also demonstrated in the literature. Figure 8 shows the stress–strain curves obtained from uniaxial compression–decompression tests on these aerogels. In addition to the increase in compressive stress accompanied by an increase in bulk density, an increase in the resilience after unloaded can be observed. Since a distinct improvement concerning resilience cannot be observed in the aerogels such as PVSQ-TGA (Fig. S8), this increased resilience is presumably related to increased crosslinking density. In order to confirm a successful progress of the thiol-ene reactions, Raman spectroscopy was employed, results of which are shown in Fig. S9. Apparently, substantial changes in the shape of peaks are observed in the region colored with red (ca. 2800–3100 cm^{-1}). These changes involve the decrease in the peak at 3060 cm^{-1}, corresponding to C=C bonds of vinyl groups [35], and the increase in the peaks around 2800–2940 cm^{-1}, which can be assigned to CH_2 symmetric or asymmetric stretching vibrations [36]. Changes are also observable in the region colored with green (650–800 cm^{-1}), which can be attributed to C−S (ca. 650 cm^{-1}) and CH_2 rocking vibrations, and blue (around 1600 cm^{-1}), corresponding to C=C bonds. Since there are only small peaks around 2575 cm^{-1}, corresponding to S−H bonds, most of the thiols are consumed

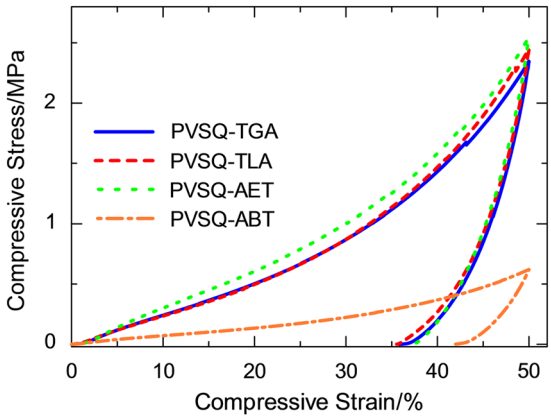

Fig. 8 Stress–strain curves obtained from uniaxial compression–decompression tests on aerogels underwent thiol-ene reactions using dithiols

by the thiol-ene reactions, contributing to the higher crosslinking density.

3.6 Hydrosilylation reactions

Applicability of hydrosilylation onto the pendant vinyl groups was briefly investigated. Since hydrosilylation produces a stable C−C bond between a double-bond carbon atom and an Si−H moiety, chemical stability of the attached parts is higher than thiol-ene reactions, which form less stable C−S bonds. Hydrosilylation is generally used in surface modifications on such as hydride-passivated porous silicon [37–39]. However, the number of reports on hydrosilylation onto the vinyl groups in a porous solid matrix is strictly limited. In the present work, TPS was utilized as a silylating agent. Figures 9a and b show the appearance of the aerogel that underwent hydrosilylation with TPS (PVSQ-TPS). Apparently, the outer part of PVSQ-TPS is transparent with light-brown color, and the inner part is opaque. This inhomogeneous appearance is presumably caused by gradient of efficiency of the hydrosilylation reaction. Figure 9c shows Raman spectra of pristine PVSQ (PVSQ-sta) and the core part and the surface part of PVSQ-TPS. In the spectrum of the surface part, a strong peak can be observed at 992 cm^{-1}, which is assigned to C−C ring vibration [35]. The assignment of a broad peak around 1095 cm^{-1} is obscure; however, peaks corresponding to C−H ring vibration appear around 1120 cm^{-3} [35], which may contributed to the broad peak in the spectrum. On the other hand, the spectrum of the core part only shows small peak at 992 cm^{-1}, and the shape of the other peaks are mostly identical to that of pristine PVSQ. The yield of hydrosilylation is therefore largely decreased from the surface to the core of the PVSQ-TPS aerogel. A similar phenomenon has been reported in surface-modified silica

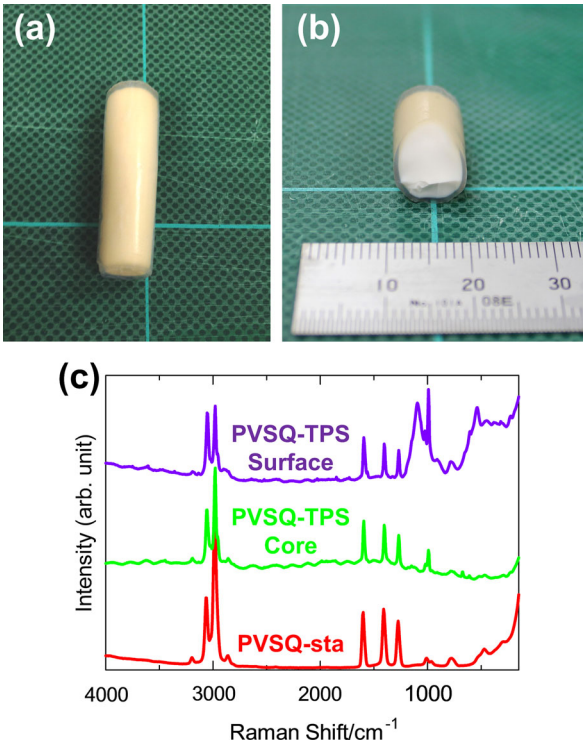

Fig. 9 **a** Appearance, **b** a cross section of PVSQ-TPS aerogel. **c** Raman spectra of PVSQ-sta and a core part and a surface of PVSQ-TPS

aerogels using reversible addition-fragmentation chain transfer polymerization [40]. Due to small pores where catalyst and reactant cannot be homogeneously dispersed with ease, vinyl groups located near the macroscopic surface of the gel can react with TPS more easily than those located near the core. Because of the increased bulk density (0.21 g cm^{-3}), compressive stress at 50% strain is increased (Fig. S10), compared to those of pristine PVSQ aerogels as displayed in Fig. 2d. However, the resilience after unloaded is similar to those of pristine PVSQ (typically ca. 60%), and this is the case similar to the thiol-ene reaction using a monofunctional thiol such as TGA. From a weight loss during thermogravimetry, the yield of the hydrosilylation reaction is estimated as ca. 1.4% (data from a round slice specimen containing both surface and core parts). Still further optimization required, here we showed the possibility of hydrosilylation onto the vinyl groups in a solid matrix of transparent porous materials.

4 Conclusions

We have systematically investigated effects of synthetic conditions on the properties of resultant PVSQ aerogels, particularly focusing on their visible-light transparency.

Concentration and cation species of the base catalyst strongly affect light transmittance of resultant aerogels. Aerogels prepared using TMAOH, choline hydroxide or THMAOH leads to higher transmittance as compared to those using alkali metal hydroxides and other tetraalkylammonium hydroxides. Concerning gelation and aging conditions, it is important to employ appropriate temperature and duration in order to obtain high transparency of resultant aerogels. Too high temperature and too long aging duration end up in lowering the light transmittance and surface area. By optimizing the amount of liquid surfactant, light transmittance of aerogels reaches as high as 70% (at a wavelength of 550 nm for a 10-mm thick sample). With respect to acid catalyst, higher concentration results in lower light transmittance.

Applicability of post-modification via thiol-ene reactions and hydrosilylation has also been investigated. In the case of thiol-ene reactions, several compounds are shown to be effective to modify surface hydrophobicity/hydrophilicity and mechanical properties. Hydrosilylation did not homogeneously take place in a whole gel body in the centimeter scale; however, it successfully proceeded near the bulk surface of the gel, confirmed by Raman spectroscopy. These addition reactions are highly potential for imparting further functionalities on transparent PVSQ aerogels.

Acknowledgements The present study has been performed under financial support from Advanced Low Carbon Technology Research and Development Program (ALCA, Japan Science and Technology Agency).

References

1. Hüsing N, Schubert U (1998) Aerogels-airy materials: chemistry, structure, and properties. Angew Chem Int Ed 37:22–45
2. Alexander S (1989) Vibrations of fractals and scattering of light from aerogels. Phys Rev B 40:7953–7965
3. Cao W, Hunt AJ (1994) Improving the visible transparency of silica aerogels. J Non-Cryst Solids 176:18–25
4. Baetens R, Jelle BP, Gustavsen A (2011) Aerogel insulation for building applications: a state-of-the-art review. Energy Build 43:761–769
5. Maleki H, Durães L, Portugal A (2014) An overview on silica aerogels synthesis and different mechanical reinforcing strategies. J Non-Cryst Solids 385:55–74
6. Kanamori K, Aizawa M, Nakanishi K, Hanada T (2007) New transparent methylsilsesquioxane aerogels and xerogels with improved mechanical properties. Adv Mater 19:1589–1593
7. Kanamori K, Aizawa M, Nakanishi K, Hanada T (2008) Elastic organic-inorganic hybrid aerogels and xerogels. J Sol Gel Sci Technol 48:172–181
8. Kanamori K, Nakanishi K, Hanada T (2009) Sol-gel synthesis, porous structure, and mechanical property of polymethylsilsesquioxane aerogels. J Ceram Soc Jpn 117:1333–1338
9. Nakanishi K, Kanamori K (2005) Organic-inorganic hybrid poly (silsesquioxane) monoliths with controlled macro- and mesopores. J Mater Chem 15:3776–3786
10. Loy DA, Baugher BM, Baugher CR, Schneider DA, Rahimian K (2000) Substituent effects on the sol-gel chemistry of organotrialkoxysilanes. Chem Mater 12:3624–3632
11. Rao AV, Bhagat SD, Hirashima H, Pajonk GM (2006) Synthesis of flexible silica aerogels using methyltrimethoxysilane (MTMS) precursor. J Colloid Interface Sci 300:279–285
12. Dong H, Brook MA, Brennan JD (2005) A new route to monolithic methylsilsesquioxane: gelation behavior of methyltrimethoxysilane and morphology of resulting methylsilsesquioxanes under one-step and two-step processing. Chem Mater 17:2807–2816
13. Kanamori K (2014) Monolithic silsesquioxane materials with well-defined pore structure. J Mater Res 29:2773–2786
14. Hayase G, Kugimiya K, Ogawa M, Kodera Y, Kanamori K, Nakanishi K (2014) The thermal conductivity of polymethylsilsesquioxane aerogels and xerogels with varied pore sizes for practical application as thermal superinsulators. J Mater Chem A 2:6525–6531
15. Shimizu T, Kanamori K, Maeno A, Kaji H, Doherty CM, Falcaro P, Nakanishi K (2016) Transparent, highly insulating polyethyl- and polyvinylsilsesquioxane aerogels: mechanical improvements by vulcanization for ambient pressure drying. Chem Mater 28:6860–6868
16. Brook MA (2000) Silicon in organic, organometallic, and polymer chemistry. Wiley, New York, NY
17. Scherer GW (1992) Stress development during supercritical drying. J Non-Cryst Solids 145:33–40
18. Zhu Y, Morimoto Y, Shimizu T, Morisato K, Takeda K, Kanamori K, Nakanishi K (2015) Synthesis of hierarchically porous polymethylsilsesquioxane monoliths with controlled mesopores for HPLC separation. J Ceram Soc Jpn 123:770–778
19. Reichenauer G, Scherer GW (2001) Extracting the pore size distribution of compliant materials from nitrogen adsorption. Colloids Surf A 187-188:41–50
20. Shimizu T, Kanamori K, Maeno A, Kaji H, Nakanishi K (2016) Transparent ethylene-bridged polymethylsiloxane aerogels and xerogels with improved bending flexibility. Langmuir 32:13427–13434
21. Ishida H, Koenig JL (1978) Fourier transform infrared spectroscopic study of the silane coupling agent/porous silica interface. J Colloid Sci 64:555–564
22. Hæreid S, Anderson J, Einarsrud MA, Hua DW, Smith DM (1995) Thermal and temporal aging of TMOS-based aerogel precursors in water. J Non-Cryst Solids 185:221–226
23. Brinker CJ, Scherer GW (1990) Sol–gel science: The physics and chemistry of sol–gel processing. Academic, San Diego, CA, Chapter 4
24. Dong H, Brennan JD (2006) Macroporous monolithic methylsilsesquioxanes prepared by a two-step acid/acid processing method. Chem Mater 18:4176–4182
25. Hayase G, Kanamori K, Nakanishi K (2012) Structure and properties of polymethylsilsesquioxane aerogels synthesized with surfactant *n*-hexadecyltrimethylammonium chloride. Microporous Mesoporous Mater 158:247–252
26. Lowe AB (2010) Thiol-ene "click" reactions and recent applications in polymer and materials synthesis. Polym Chem 1:17–36
27. Wang Z, Dai Z, Wu J, Zhao N, Xu J (2013) Vacuum-dried robust bridged silsesquioxane aerogels. Adv Mater 25:4494–4497
28. Nischang I, Brüggemann O, Teasdale I (2011) Facile, single-step preparation of versatile, high-surface-area, hierarchically structured hybrid materials. Angew Chem Int Ed 50:4592–4596
29. Hayase G, Kanamori K, Hasegawa G, Maeno A, Kaji H, Nakanishi K (2013) A superamphiphobic macroporous silicone monolith with marshmallow-like flexibility. Angew Chem Int Ed 52:10788–10791
30. Brozek EM, Zharov I (2009) Internal functionalization and surface modification of vinylsilsesquioxane nanoparticles. Chem Mater 21:1451–1456

31. Cui S, Cheng W, Shen X, Fan M, Russell AT, Wu Z, Yi X (2011) Mesoporous amine-modified SiO_2 aerogel: a potential CO_2 sorbent. Energy Environ Sci 4:2070–2074
32. Van Humbeck JF, McDonald TM, Jing X, Wiers BM, Zhu G, Long JR (2014) Ammonia capture in porous organic polymers densely functionalized with Brønsted acid groups. J Am Chem Soc 136:2432–2440
33. Meador MAB, Weber AS, Hindi A, Naumenko M, McCorkle L, Quade D, Vivod SL, Gould GL, White S, Deshpande K (2009) Structure-property relationships in porous 3D nanostructures: epoxy-cross-linked silica aerogels produced using ethanol as the solvent. ACS Appl Mater Interfaces 1:894–906
34. Nguyen BN, Meador MAB, Tousley ME, Shonkwiler B, McCorkle L, Scheiman DA, Palczer A (2009) Tailoring elastic properties of silica aerogels cross-linked with polystyrene. ACS Appl Mater Interfaces 1:621–630
35. Capeletti LB, Baibich IM, Butler IS, dos Santos JHZ (2014) Infrared and Raman spectroscopic characterization of some organic substituted hybrid silicas. Spectrochim Acta Part A 133:619–625
36. Bryant MA, Pemberton JE (1991) Surface Raman scattering of self-assembled monolayers formed from 1-alkanethiols: behavior of films at Au and comparison to films at Ag. J Am Chem Soc 113:8284–8293
37. Buriak JM (2002) Organometallic chemistry on silicon and germanium surfaces. Chem Rev 102:1271–1308
38. Stewart MP, Buriak JM (1998) Photopatterned hydrosilylation on porous silicon. Angew Chem Int Ed 37:3257–3260
39. Rogozhina EV, Eckhoff DA, Gratton E, Braun PV (2006) Carboxyl functionalization of ultrasmall luminescent silicon nanoparticles through thermal hydrosilylation. J Mater Chem 16:1421–1430
40. Maleki H, Durães L, Portugal A (2015) Synthesis of mechanically reinforced silica aerogels *via* surface-initiated reversible addition-fragmentation chain transfer (RAFT) polymerization. J Mater Chem A 3:1594–1600